Deconvolved SWI phase model of patients with Parkinson disease

G. Grabner[1,2], S. Trattnig[1], and M. Barth[2]

[1]Department of Radiology, Medical University of Vienna, Vienna, Austria, [2]Donders Institute for Brain, Cognition and Behaviour, Radboud University Nijmegen, Nijmegen, Netherlands

Introduction: Transverse MR relaxation times are a marker of increased iron deposition and therefore a possible indication for Parkinson disease (PD) [1]. In principle, the MR phase image should reflect the magnetic susceptibility of tissues and – hence – iron concentration more directly, but the phase image is actually the convolution of the susceptibility carrying volumes with the typical pattern of a magnetic dipole [2]. This leads to very complex spatial phase patterns especially in the case of intricate geometrical shapes, as e.g. the various nuclei of the basal ganglia. This complicates the definition of regions of interest (ROIs) on phase data itself and ROI definition on magnitude data is undesired due to inclusion of additional effects. In the phase image the nature of the dipolar kernel leads to dramatic phase changes in the vicinity of tissue borders which make the estimated phase value critically dependent on the ROI definition. Here we propose a novel procedure to analyse MR phase images that applies a filtered deconvolution on a group specific phase model to reduce this dipole effect and to simplify ROI definition.

Material and Methods: MRI: T1 weighted and SWI data from 27 Parkinson's (PD) patients were acquired on a 3 Tesla whole body MR scanner (Siemens, Erlangen, Germany) with a 12 channel head coil. A three-dimensional, fully first-order flow-compensated gradient-echo (SWI) sequence with a TE of 29ms was used for SWI. Other sequence parameters were: TR = 36ms; image-matrix = 256x256 pixel; slices = 176; GRAPPA factor = 2, TA = 17:22 min, resolution = 0.8 mm isotropic. The SWI phase images were filtered using a Homodyne filter with a Gaussian filter kernel corresponding to a fwhm 5mm in image space. T1 weighted imaging parameters were: sagittal MPRAGE with 208 slices, TR/TI/TE 2300/900/3.59 ms, image-matrix = 320x320, resolution = 0.8mm^3; TA = 12:18 minutes.

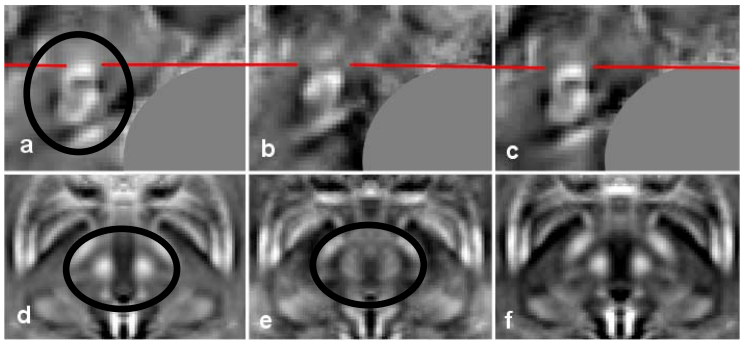

Fig. 1: (a,b,c) sagittal slices through the RN (circle) within the phase model (a), the deconvolved phase model (b) and the convolved-deconvolved phase model (c). (d,e,f) represent an axial slice through basal ganglia, just above the RN marked with a red line on the sagittal images. Note the dipole effect in the phase model (circle). The phase model (a,d) and the convolved-deconvolved phase model (c,f) for the RN are very similar indicating a small masking effect for the RN. The largely reduced dipole effect in the deconvolved phase model (b,e) compared to (a,d) or (c,f) enables ROI definition with higher accuracy.

Phase Model and Deconvolution: In order to perform deconvolution, a high SNR phase model representing the average of the 27 PD patients was built using the method introduced by Grabner et al. [3]. In brief, this method involves linear and stepwise non-linear registration of T1–weighted subject data to an evolving model. Here, registration transformations used to create a T1–weighted model were applied to filtered SWI phase data in order to create a phase model. Transformations created with T1–weighted data – rather than phase – were used to create the phase model due to the problematic phase patterns that can cause non-linear image registration to fail. Deconvolution was performed using

$$phase_{deconv} = F^{-1}\left(\frac{F(phase_{model})}{F(dipole)} * s\right)$$

where F represents the Fourier transform and s a mask in frequency space. s was designed to address the noise amplification problem where F(dipole) is close to zero and was set to 1 for F(dipole)>SD(abs(F(dipole))) and to 0 for the rest. In order to visualize the effect of masking in frequency space the deconvolved phase model was again convolved without masking. Mean phase values and standard deviations for the red nucleus (RN), the substantia nigra (SN), the putamen (PUT) and the globus pallidus (GP) were calculated from the phase model by using ROIs defined within the deconvolved phase model (except the SN, which was defined on the phase model because of the massive dipole effect) and were compared to results obtained from the individual data-sets (ROIs were automatically predefined by using model based segmentation and manually corrected).

Results: Fig. 1 shows the performance of deconvolution and the effect of the masking in frequency space. Filtered phase data and deconvolved phase data are compared to magnitude data in Fig. 2. Determined mean phase values and SD for different nuclei are presented in Tab. 1. Mean phase values for both methods (obtained from model and from individual subject data-sets) are in good agreement but the SD for model analysis is clearly reduced. The values for the RN and the PUT are in good agreement with data from healthy volunteers [4], whereas the phase values for the SN and the GP are roughly doubled which is in line with an increase of iron storage associated with Parkinson disease.

	Phase Model		Individual Data-Sets	
	Phase (ppm)	Phase (SD)*	Phase (ppm)	Phase (SD)**
RN	0.022	0.018	0.024	0.04
SN	0.045	0.012	0.040	0.035
GP	0.024	0.019	0.022	0.043
PUT	0.019	0.024	0.021	0.048

Tab. 1: Calculated mean phase values an SD; * SD of ROI phase values; ** mean of the subject specific SD of phase values.

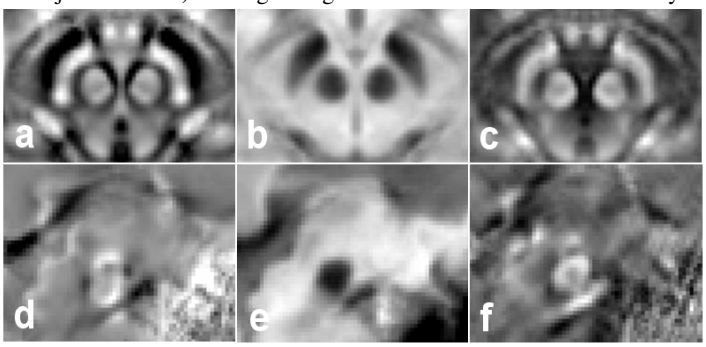

Fig. 2: Filtered phase (a,d) and deconvolved phase data (c,f) compared to magnitude data (b,e). Note the much better anatomical agreement between deconvolved and magnitude data than between phase and magnitude data.

Discussion and Conclusion:

This work demonstrates that filtered deconvolution of averaged SWI phase data is possible and leads to a more accurate phase value estimation. Furthermore, phase analysis on a group specific model decreases the tracing effort as only one data set per subject/patient group has to be defined instead of one per subject.

References:

1) Gorell JM. et al. Neurology 1995 Jul;45(7):1420.

2) Pathak AP. et al. Neuroimage. 2008 Apr 15;40(3):1130-43.

3) G. Grabner et al. MICCAI 2006, volume II : 58–66

4) Haacke EM. et al. J Magn Reson Imaging. 2007 Aug;26 (2):256-264.